Cluster-GMC Encounters

Computational Astrophysics - Final Project

Saeid Mahmoudzadeh - s2547341, Yuan Chen - s2562081
Christiaan van Buchem - s1587064

December 10, 2019

1 Introduction

It is estimated that there are 125 globular clusters to be found in and around our milky-way (Murdin, 2001). These clusters have highly eccentric orbits around the galactic center with a relative velocity of about $100 - 300$ km/s and periods of up to 800 million years. As these clusters orbit the galactic center and pass through the galactic disk, they must pass through the interstellar gas spread throughout our galaxy (Dame et al., 2001). For our final assignment for the Computational Astrophysics course, we decided to investigate what would occur if globular cluster were to collide with a giant molecular cloud and if this could trigger star formation within the cloud. In this report we will be presenting how we investigated this scenario using Amuse. After the introduction we will be presenting our method in the section following our introduction, we will then show our results. Finally we will then discuss our results and draw our conclusions. However, we will first begin by giving some more background information on the subject in this introduction.

Wallin et al. (1996) and Levy (2000) have shown that a globular cluster passing through the plane of the milky-way can trigger star-formation in the gaseous disk. Research has also been carried out by Lamers et al. (2005) and Gieles et al. (2006) and used N-body simulations and analytical equations in order to show that star clusters tend to be broken up in the potential fields of galaxies and massive GMCs. Sometime later Murray et al. (2010) and Murray (2011) have shown when one takes ionization and radiation effects into account, using radiative-magneto-hydrodynamic codes, clusters can trigger star-formation in GMCs. What we investigate in this project is whether or not the interaction between a globular cluster and a GMC can trigger star-formation purely through the gravitational interaction, excluding the effects from ionization and radiation. Since globular clusters are generally composed of very old stellar populations (Murdin, 2001), radiative pressure should have less influence on the cloud in this scenario (Wallin et al., 1996). The manner in which we will do to test whether star formation could occur is by looking at the effect that a cluster has on the density distribution of a GMC and seeing if there are any points where Jeans' criterion is satisfied. We hypothesise that the collision between a GMC and a star cluster of similar mass could trigger star formation within the GMC under some circumstances.

2 Method

In this section we will be covering the manner in which we set-up our experiment. This consists of an overview of the code that we used, the diagnostics that we kept in order to track what is happening in each set-up and the initial conditions that we tested.

2.1 The codes

All of the simulation code used for this project was included in Amuse (Portegies Zwart et al., 2019). The main code that we used for this project is the smoothed particle hydrodynamic (sph) code named `Fi`. In our initial set-up used the bridge function build in to Amuse in order to join this code with an N-Body integrator, `ph4`, which we used to integrate the motion of the stars within the cluster. However, we found that this resulted in unrealistic behaviour of the GMC. Similarly to the issue that we encountered in assignment 4 of this same course, it appeared that the size of the bridge step between the two codes was too large causing the particles in the sph code to 'drift' for too long which caused unexpected behaviour. For instance, we added a massive star at rest somewhere inside the GMC. Using bridge between the gravity code for the star and the hydro code for the GMC made the GMC to dissipate as Figure 1.

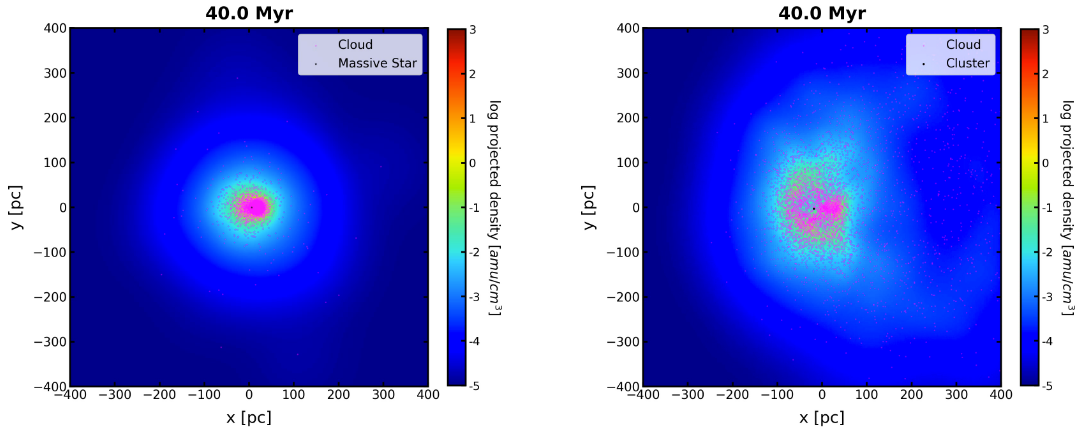

(a) SPH

(b) Bridge between gravity and SPH

Figure 1: Here we can see the snapshot of the simulation after 40 Myr evolution of the GMC and the massive star using (a) hydro code and (b) bridge between the gravity and hydro code.

2.2 Initialization of the cloud and the cluster

In order to determine what initial parameters we wanted to use for our experiment we based it as much as possible on what we could potentially encounter in nature as well. Once we decided upon an initial experimental set-up, we varied those parameters for different experiments (see Table 1). In this subsection we will give an overview of how we came upon our initial values for both the cluster and the cloud. In the results section we will also show some data we gathered from evolving the systems separately so as to show what their behaviour is like when they are isolated (giving us a baseline with which to compare our other results).

Cluster: Globular clusters typically contain 10^4 up to 10^6 stars and have diameters of about $5 - 200$ parsec. Due to the fact that we were also limited in terms of computation power, we decided that take the lower end of the spectrum and to test our clusters with values around 1×10^4 stars with $2M_\odot$ per star, and a virial radius of about 3 parsec (the full radius is about 20-30 parsec). For the initialisation of the cluster we used a virialized plummer model (Plummer, 1911), available in AMUSE in the function called `gasplummer.new_plummer_model()`. For the initial mass distribution, we used a power-law mass function `new_powerlaw_mass_distribution` with the power law index $\alpha = -2.35$. The cluster's initial position (in the x,y plane) relative to the cloud was set to $-200, -200$ parsec and the initial velocity was $3km/s$ in both the x and y direction.

Cloud: Typically GMCs have masses of $10^4 - 10^6 M_\odot$ and sizes of 50-200 parsec (Dame et al., 2001). Hence we decided to test for values around $M_{\rm tot} = 1 \times 10^5 M_\odot$ (5×10^4 particles, $2M_\odot$ each) and $R_{\rm vir} = 10$ pc. Initially we used a custom AMUSE function named `molecular_cloud()` to generate the cloud, however this kind of clouds are not virialized and therefore became unstable throughout the simulation. This is illustrated in Figure 2. Depending on the initial conditions, the clouds would either collapse or disperse after a number of time steps. We therefore decided that this would not be a suitable way to test the effect of globular clusters on the GMCs and opted for initializing the GMC using a plummer model as well.

2.3 Time step

There are two time steps in our program: the time step for evolving the `sph` code (`dt_sph`) and the diagnostic time step (`dt_diag`) for saving data, making plots, and resolving potential star formation and merging events. Initially, we set `dt_sph` = 0.1 Myr and `dt_diag` =1.0 Myr, but we also considered potential changes in the evolving time step to keep the simulation as accurate as

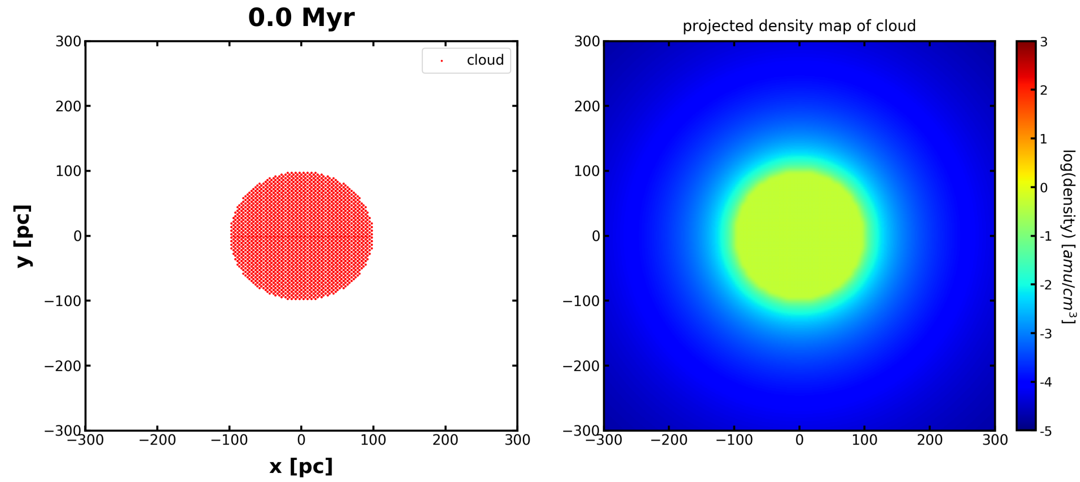

(a) The simulated GMC produced when using `molecular_cloud()` at $t = 0$.

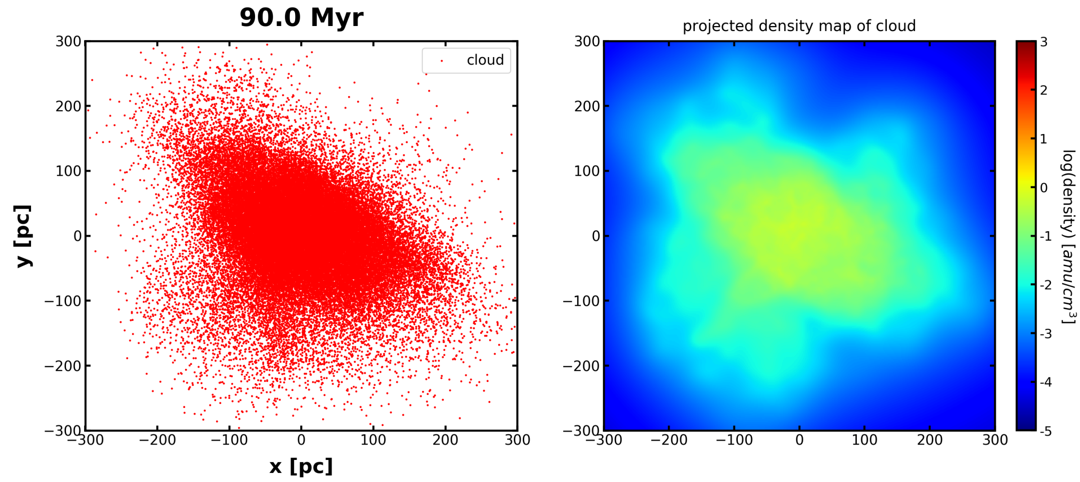

(b) The simulated GMC produced when using `molecular_cloud()` after evolving at $t = 90$ Myr.

Figure 2: Here we can see the difference between a molecular cloud after having just generated it and after having evolved it for 90 Myr. It is clearly not stable.

we could: in each diagnostic step, we calculated the dynamical, relaxation, and free-fall timescales for both the cluster and the cloud, and update the evolving time step `dt_sph` to be 1/10 of the shortest timescale. The running output showed that `dt_sph` would be around 0.03 Myr at most of the cases.

2.4 Jeans' criterion and star formation

Generally, the study of star formation is based on the competition between gravitation attraction and different dispersing processes. The most well known criterion for gravitational collapse goes back to Jeans (1902), who studied the stability of self-gravitating isothermal gas-spheres. He found that if the density of a given part of gas cloud exceeds the critical density D_J, gravity overwhelms pressure gradients and the system collapses. D_J is given by the following equation:

$$D_J = \frac{81 k_B^3}{32\pi G^3} \frac{T^3}{m^3 M^2} \tag{1}$$

Where k_B is the Boltzmann constant, G the gravitational constant, m the average mass of a gas particle, M the mass of the cloud and T the temperature. This is the criterion that we used to determine if a section of the cloud would collapse into a star. We implemented this by selecting out those gas particles in the `sph` code whose density was greater than D_J in each diagnostic step. Each of these high-density particles was then turned into a star and added into the dark-matter particle set of the `sph` code. The star inherited the mass of the gas particle, but its radius was recalculated according to the mass-radius relation for zero-age main-sequence stars (ZAMS), since the radius of a gas particle is usually too large (in an order of 1 pc) to be assigned to a star.

In practice, we calculated the Jeans' density for each of the gas particles. The cloud mass M was replaced by the mass of a single gas particle, and m was estimated as the mass of a molecular hydrogen ($2 \times 1.667 \times 10^{-27}$ kg). For the temperature T, we fixed it to be 15 K, which is a typical value for molecular clouds. We did try calculating the temperature using the ideal gas law

$$p = \rho R_d T \tag{2}$$

where p, ρ, and T are the pressure, density, and temperature of gas particles, respectively. R_d is the specific gas constant, for which we used the value of molecular hydrogen 4124.2 J/(kg·K). However, the temperature derived in this way was of a magnitude of 10^3 K, which was far higher than what we expected for a molecular cloud. We checked the density distribution of the gas particles in the cloud, and found the value ranged from 1×10^{-19} to 1×10^{-17} kg/m^3, which was comparable to the observational data (Murdin, 2001). Considering that ρ and R_d were of reasonable values, we suspected that it was something wrong with the gas pressure, probably because that the Plummer model has a large dense core in the center, in which the gas pressure is too high to resemble the actual environment in molecular clouds. Although a high gas pressure was likely to affect the reliability of our simulation, we did not find a better solution rather than kept the temperature to be 15 K when calculating the Jeans' density.

2.5 Star merging

We also considered the case of star merging when two stars are too close to each other. In each diagnostic step we picked out those star pairs in which the distance between its two members is smaller than `merge_radius`. We tried different values of this parameter and found that star merging events would happen only when `merge_radius` was greater than 0.01 pc ($\sim 2 \times 10^3$ au), which was unrealistically large as far as we were concerned. Therefore, we kept relevant functions in our code but turned them off throughout our project.

3 Results

Table 1: Overview of the different experimental set-ups. We fixed the virial radii of the cloud and the cluster as **10 pc** and **3 pc**, respectively. The number of gas particles and stars also remained unchanged (N_{gas} = 50000, N_{star} = 10000) except for the last Run. The explored parameters were the total mass of the cloud and the cluster (M_{cloud} & $M_{cluster}$), the power law index of the mass distribution of the cluster α, and the initial velocity of the cluster $\mathbf{v_0}$. The last column indicates whether star formation is triggered during the simulation. Run 0 is our very first trial, but Run 3 is the actual control group (in bold). In every other run we changed only one parameter (in red). Note that in Run 5 the direction of $\mathbf{v_0}$ was specified to give an impact parameter of b = 40 pc, while in other runs it was a head-on collision with $b = 0$.

Run	$\mathbf{M_{cloud}}$ [$M_\odot$]	$\mathbf{N_{gas}}$	$\mathbf{M_{cluster}}$ [$M_\odot$]	$\mathbf{N_{star}}$	α	$\mathbf{v_0}$ [km/s]	**SF?**
1	1×10^5	5×10^4	2×10^4	1×10^4	-2.35	(3, 3, 0)	N
2	1×10^5	5×10^4	5×10^4	1×10^4	-2.35	(3, 3, 0)	N
3	$\mathbf{1 \times 10^5}$	$\mathbf{5 \times 10^4}$	$\mathbf{5 \times 10^4}$	$\mathbf{1 \times 10^4}$	**-1.5**	**(3, 3, 0)**	**N**
4	1×10^5	5×10^4	5×10^4	1×10^4	-0.5	(3, 3, 0)	**239**
5	1×10^5	5×10^4	5×10^4	1×10^4	-1.5	(10, 10, 0)	N
6	1×10^5	5×10^4	5×10^4	1×10^4	-1.5	(3.2, 2.8, 0)	N
7	1.25×10^5	5×10^4	5×10^4	1×10^4	-1.5	(3, 3, 0)	**389**
8	1.4×10^5	7×10^4	5×10^4	1×10^4	-1.5	(3, 3, 0)	N

In this section we will present the results of our experiments, based on which we will then make some comparison and analyses. **Table 1** displays the parameters we explored in different experiments. We started with Run 0 but the values were not good enough for comparison. After several trials we finally set **Run 3** as our control group. In every experiment, we saved various kinds of data for further analyses. For the cluster, we saved the initial mass distribution of the star members; for the cloud, we saved the density maximum and the number of newly formed stars in each diagnostic step; and for both of them, we saved the Lagrange radii (the radii in which 20%, 50%, 90% of the total mass are contained) and the kinetic/potential energy every step as well. In the following sub-sections we will dive into different groups of experiments in which only one parameter was changed. [Note: after the presentation we found some bugs in our code and redid the simulations, so the results presented here would be slightly different from what we had in our slides, but the qualitative conclusions are the same.]

3.1 Total mass of the cluster (Run 1/2)

From Run 1 to Run 2 we increased the total mass of the cluster by increasing the average stellar mass from 2 $M_\odot$ to 5 $M_\odot$. From **Figure 3** we can see that a more massive cluster does result in a higher peak of the cloud density, but still not enough to reach the Jeans' density. However, the fluctuation after the 'close approach' shows that the cloud structure will be more severely affected if the cluster has more mass. This can be verified by **Figure 4** as well, in which the cloud in the bottom panel shows more dispersion at 200 Myr.

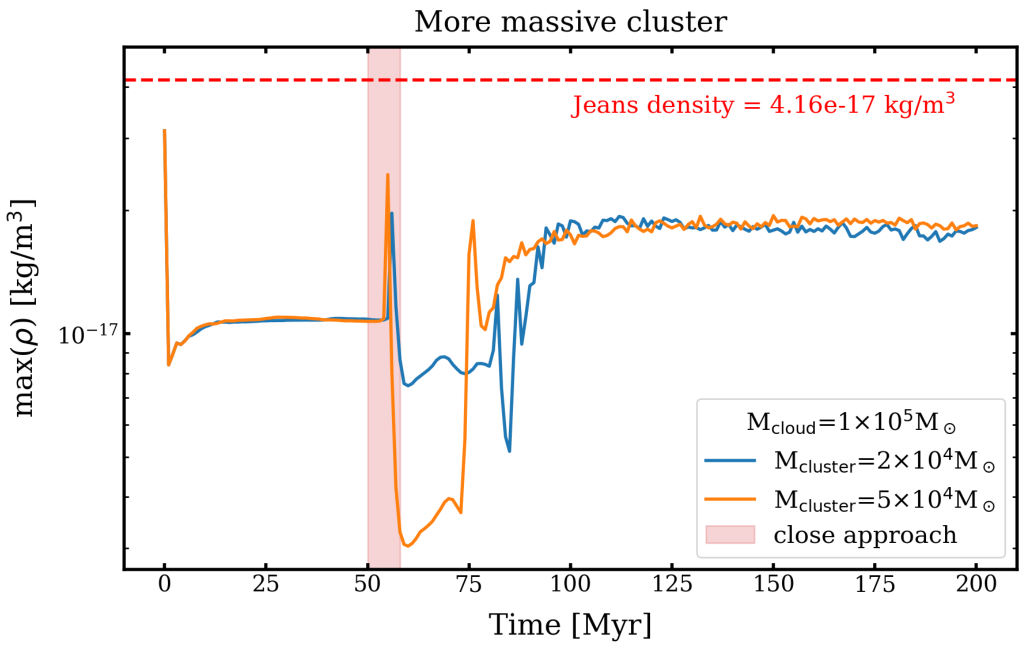

Figure 3: In this figure we can see the evolution of the maximum density of the gas particles for two different cluster masses. Note that here we can clearly see that a more massive cluster results in a higher maximum density during the collision.

You may want to ask why there are sudden 'drops' after the 'peaks'. Our conjecture is that peaks reflect some kind of shock waves in the gas, where the wave front compresses the gas and generate some high density regions. The compressing effect becomes strongest when the wave front reaches the densest region of the cloud, which is exactly the center of the Plummer sphere. However, after the wave passes through the center, the gas particles dissipate and the dense core is attenuated, therefore the maximum density drops dramatically right after the peak. But there is still a core that assembles the majority of the mass, and after some time the scattered gas particles start to gather around the diluted core (or the system tends to be re-virialized), and the maximum density goes up again. In this way we can also explain why the 'pool' is deeper when the cluster is more massive: it is because that the shock wave is more violent and the cloud is scattered more severely during the collision.

We also noticed multiple peaks in some experiments (Run 3 is already a case). From the video we can easily realize that a peak always correspond to an 'ejection' of the particles (gas or stars). And in those cases with more than two obvious peaks, there would be two obvious ejections as well. It seems that there are some intense energy exchanges during the close approach, but due to limited time resolution we are not very clear about the details yet. But these phenomena do suggest that under some circumstances there could be more than one chance to trigger star formation during the collision between clouds and clusters.

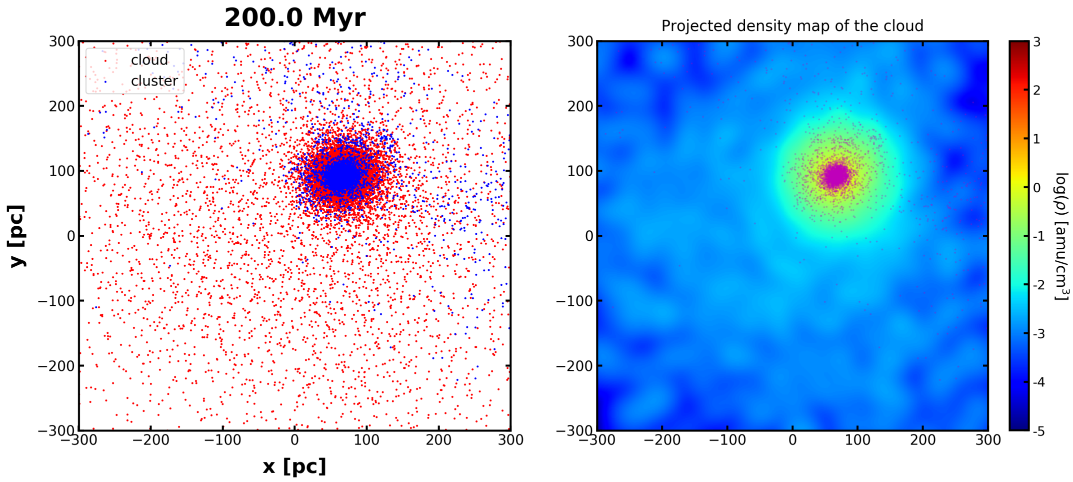

(a) Run 1 ($M_{cluster} = 2 \times 10^4 M_\odot$) at 200 Myr

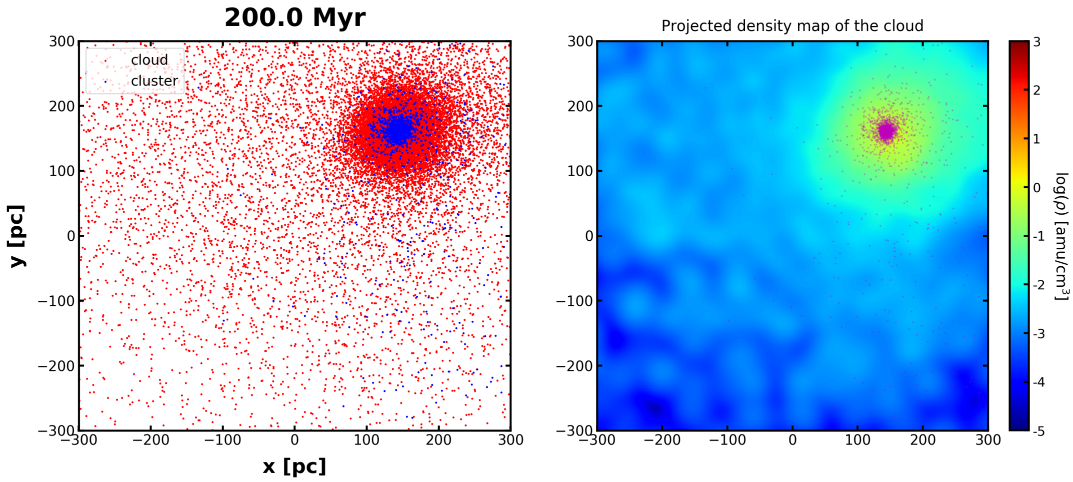

(b) Run 3 ($M_{cluster} = 5 \times 10^4 M_\odot$) at 200 Myr

Figure 4: Here we see the comparison between the cases of a normal-mass cluster and a massive cluster. The left panel shows the distribution of the gas particles (red dots) and the stars from the cluster (blue dots). The right panel is the projected density map of the cloud with some pink dots indicating the same distribution of the cluster as in the left (the color was rescaled for a better visualization). The time stamp is chosen at the end of our simulation, when the collisions have taken place for a while. We can clearly see that for the heavier cluster (bottom) the cloud is more heavily disturbed than for the lower-mass cluster.

3.2 Stellar mass distribution of the cluster (Run 2/3/4)

From now on we fixed the cluster mass at $5 \times 10^4 M_\odot$, but there is another important parameter to investigate: the power law index α of the cluster's initial mass distribution function. We tested three values of α (-2.35, -1.5, -0.5) and the mass distributions are shown in **Figure 5**. When the total mass is fixed, a larger α will lead to a smaller upper limit but increase the number of massive stars. This looks like a trade-off, but **Figure 6** shows that with a larger α the cluster does exert stronger perturbation to the cloud, especially in the case of $\alpha = -0.5$, the maximal density exceeds the Jeans' density and hence triggers star formation. This interesting result implies that even when two clusters have the same total mass, the mass distribution of their star members can make a big difference when they collide with molecular clouds. Although a cluster with $\alpha = -0.5$ does not have extremely massive stars ($M > 10^2 M_\odot$), it has substantial numbers of mid-mass stars ($M \sim 10 M_\odot$) of which the collective power is stronger than oligarchical influence.

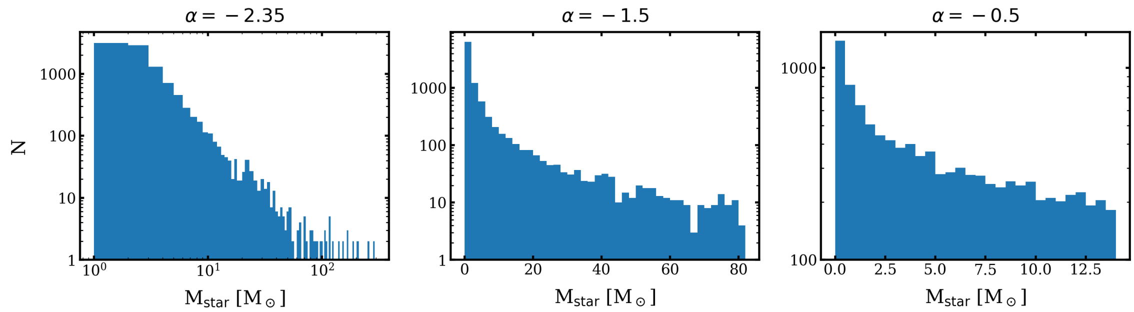

Figure 5: The mass distribution of stars in the cluster for different power-law indexes (α).

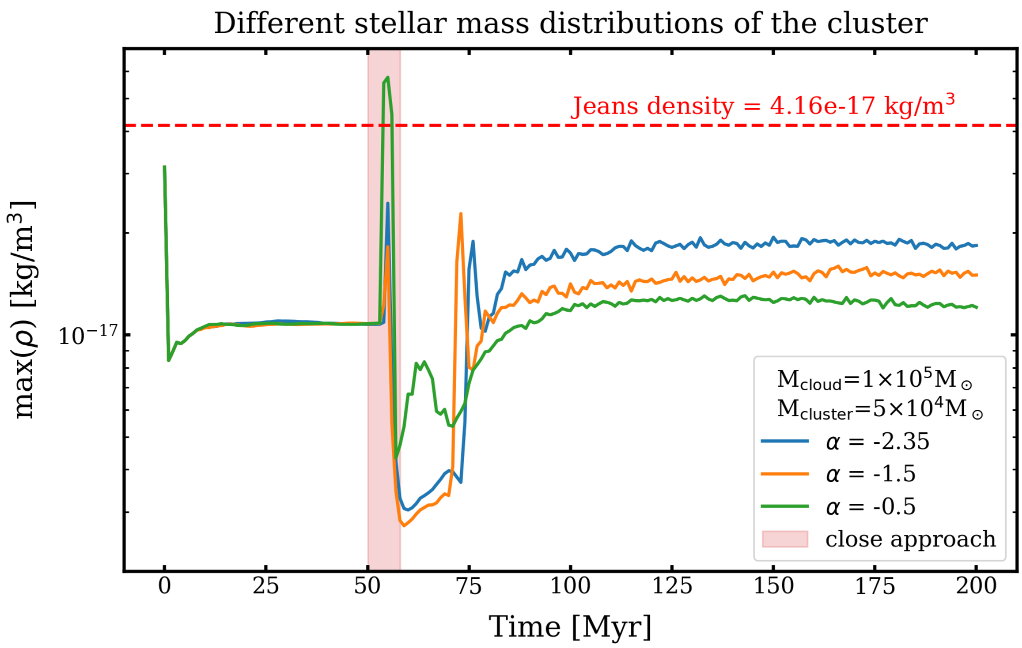

Figure 6: This plot shows the evolution of the maximum density in the cloud for different stellar mass distributions of the cluster. Note that with $\alpha = -0.5$ Jeans' criterion was satisfied.

3.3 Initial velocity of the cluster (Run 3/5/6)

In this part we discuss about how the relative velocity between the cloud and the cluster would affect their collision. Since we gave no velocity to the cloud, the initial velocity of the cluster is basically the relative velocity between them. Based on Run 3, we increased the absolute value of v_0 in Run 5 from $3\sqrt{2}$ km/s to $10\sqrt{2}$ km/s without changing its direction, so there was still a head-on collision (i.e. impact parameter $b = 0$) in Run 5. While for Run 6, we kept the absolute velocity at $3\sqrt{2}$ km/s but slightly changed its direction so that the impact parameter was 40 pc initially (say 'initially' is because that the actual closest distance between the two systems would be smaller than 40 pc due to gravitational interaction).

Figure 7 compares the evolution of maximum density of the cloud in these three experiments. We can see from the orange line that even when the collision is not completely head-on, the cluster can still cause density fluctuations in the cloud, but with a smaller magnitude. But in our previous runs shown in the presentation, we tested $b = 100$ pc and $b = 200$ pc, only to find them too large to produce noticeable effects. On the other hand, the green line (quick pass) shows that an substantial density bump can take place with a higher relative velocity.

Actually we had an experiment for $v_0 = (50, 50, 0)$ km/s in our previous runs, since the real value of v_0 should be around 10^2 km/s. But considering that other parameters in that experiment were not controlled, the data are not included here. In that case, we noticed an interesting phenomenon that there was no drop after the collision. we can also see in Figure 7 that the drop of the green line is shallower than other two lines. According to our explanation in Section 3.1, this means that the interaction between the cloud and the cluster after their collision is weaker. In **Figure 8** we can see that in the case of quick pass, the cloud does not move along with the cluster after the collision, and its shape also remains more compact. However, with a higher velocity, the density bump still exists, and its amplitude is only reduced by a little factor! This in some ways preserve the possibility of triggering star formation in a quick cloud-cluster collision, as long as the relative velocity is within some range.

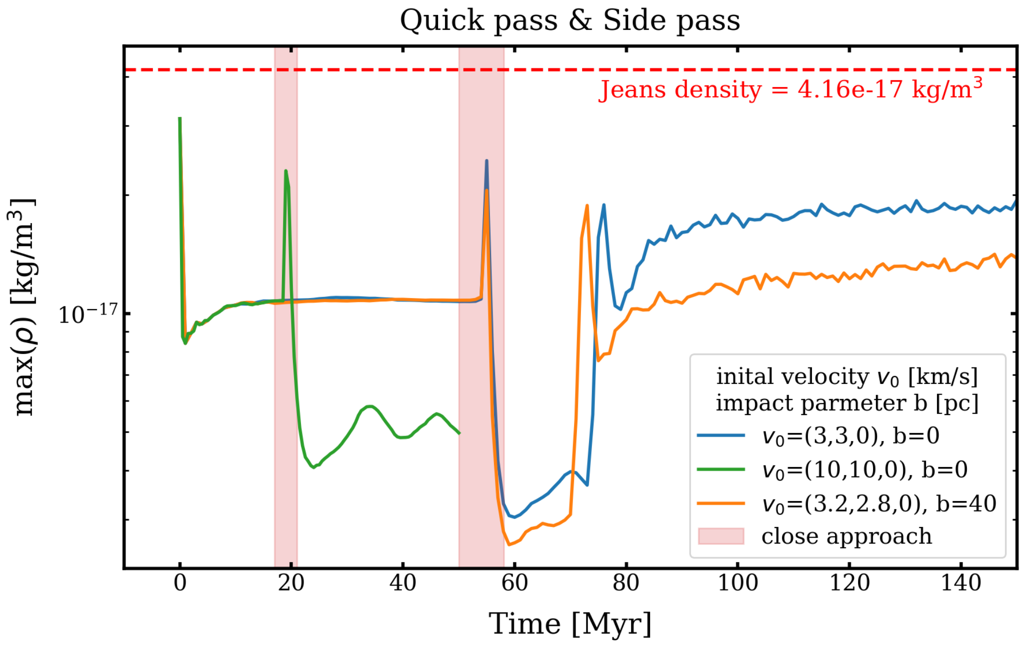

Figure 7: This figure shows the evolution of the maximum density of the GMC for different velocities and impact parameters. The red regions indicate the time windows of closest approaches. Note that a higher velocity or a larger impact parameter would give a lower maximum density peak.

3.4 Total & average mass of the cloud (Run 3/7/8)

After exploring the parameter space of the cluster, we also tried varying the initialization of the cloud. Since the gas particles in the cloud all own the same mass, we focused on the total mass and average mass of the cloud while keeping its size invariant. In Run 7 we increased the average mass of gas particles from 2 $M_\odot$ to 2.5 $M_\odot$, and in Run 8 we increased the number of gas particles from 5×10^4 to 7×10^4 . In both ways we enhanced the overall density of the cloud, but they are actually two different cases. **Figure 9** shows the comparison between Run 3 and Run 8, from which we can see that the trend of evolution is barely the same, besides that there is an overall enhancement of the cloud density in Run 8. However, the number of gas particles was still not large enough to trigger star formation in this case.

But for another case (Run 3 & Run 7), the result became different. Since the mass of each gas particles was increased, the Jeans' density of each particles would decrease according to Equation 1. In **Figure 10** we can see that the cloud with higher average mass (orange) corresponds to a lower Jeans' Density, and it was this critical decrease that enabled star formation to be triggered (twice!) in Run 7, even with a smaller total cloud mass than in Run 8. This indicates that the local stability of gas clumps in the cloud is much more important than the overall cloud mass in terms of triggering star formation.

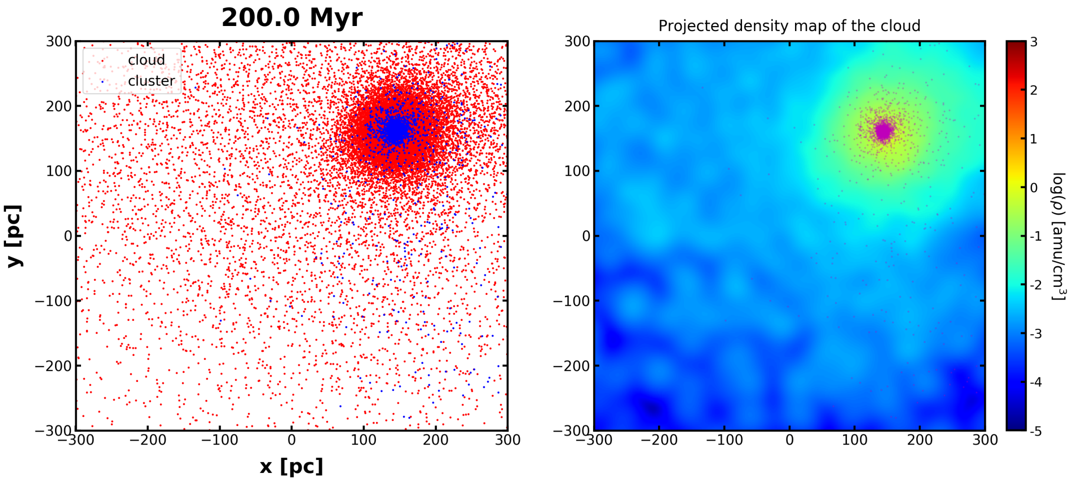

(a) Run 3 with $v_0 = (3, 3, 0)$ km/s at 200 Myr

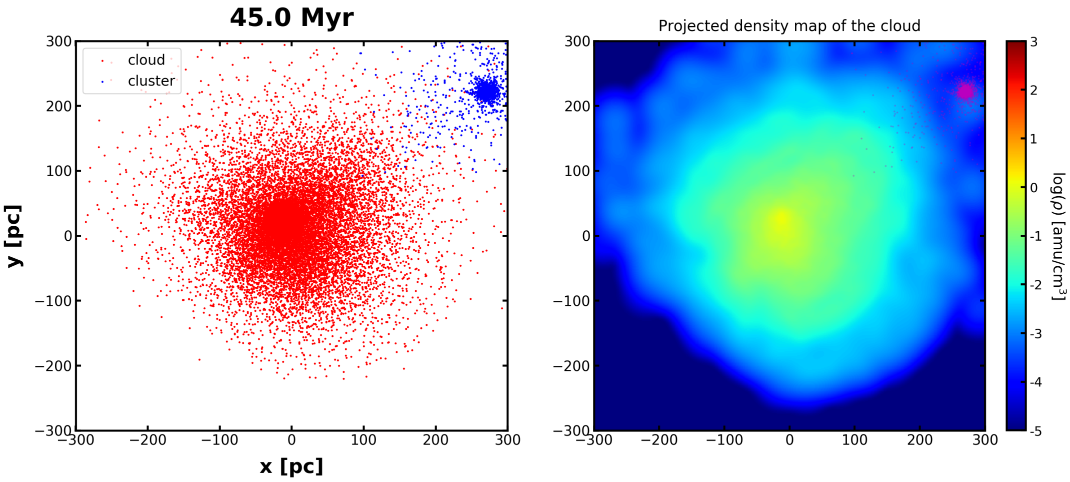

(b) Run 6 with $v_0 = (10, 10, 0)$ km/s at 45 Myr

Figure 8: Similar comparison as Fig. 4, but between different initial velocities of the cluster. The top panel is completely the same, while the bottom panel shows the snapshot at 45 Myr of a quick pass.

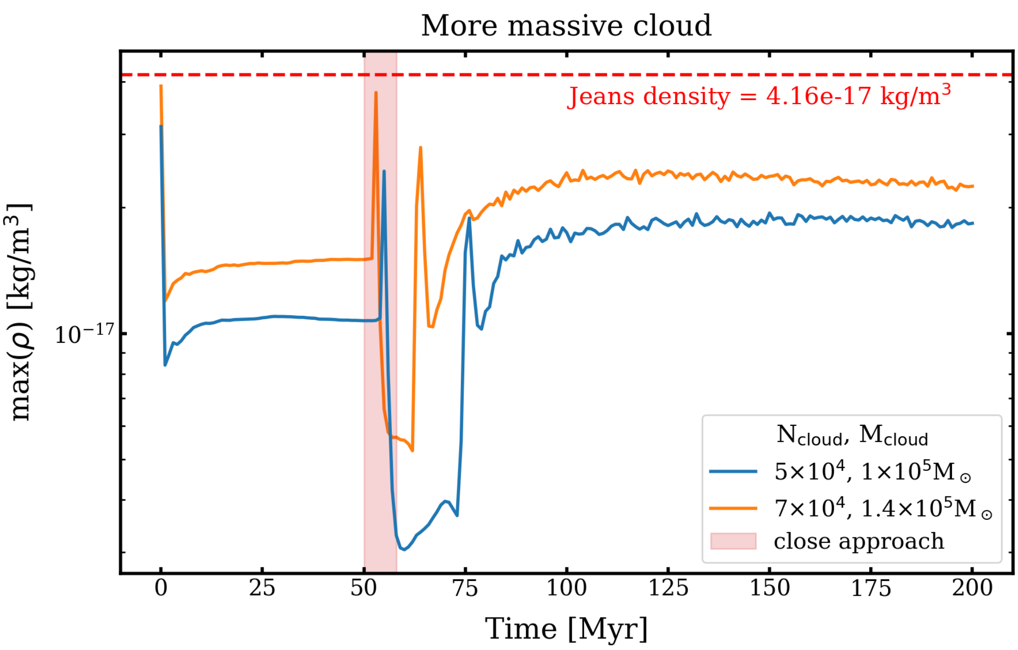

Figure 9: Here we see the evolution of the maximum density of the cloud for two different cloud masses and particle numbers.

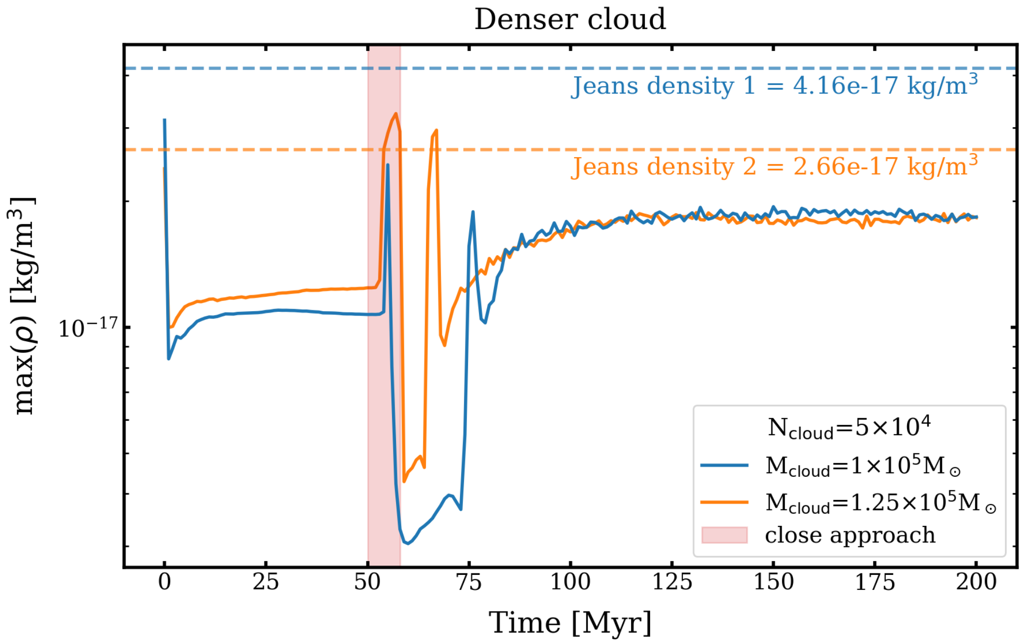

Figure 10: Here we see the evolution of the maximum density of the cloud for two different masses of gas particles, i.e. different M in Equation 1, and therefore two different Jeans' densities. The higher mass cloud managed to reach the lower Jeans' density (orange).

3.5 Evolution of Lagrange radii and energy

In order to probe what was happening during the cloud-cluster collision, we took Run 3 as an example to plot out the evolution of Lagrange radii (**Figure 11**) and energy (**Figure 12**). We checked the data from other experiments and found them also show a similar trend.

From Figure 11 we can see that only the 90% Lagrange radius increases dramatically after the close approach (denoted as red strips), while the 20% and 50% radii remain roughly their original values. This means that at least 50% of the total mass of both systems can survive the collision without being scattered out. Indeed, in all of our experiments we saw the cloud and the cluster managed to keep their sphere structure after the collisions.

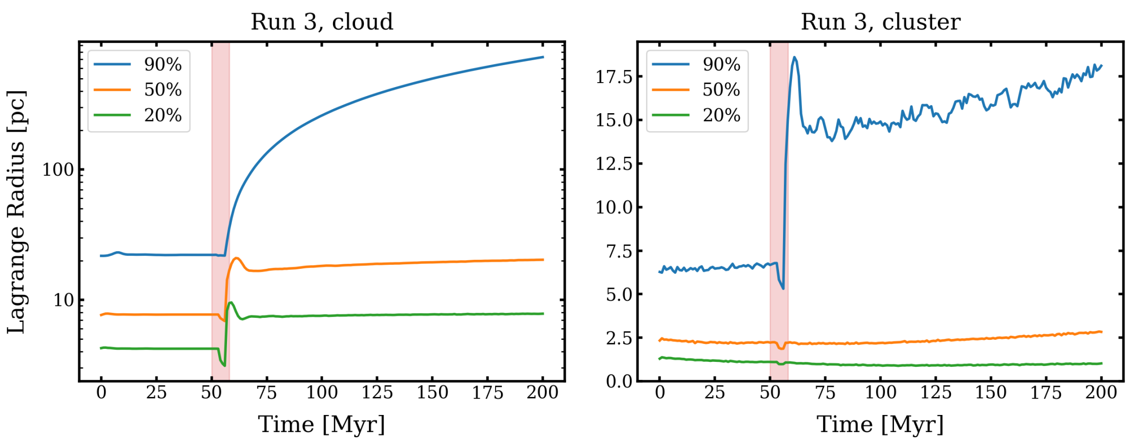

Figure 11: Evolution of Lagrange radii (20%, 50%, 90%) for the cloud (left) and the cluster (right). A 90% Lagrange radius is the radius that contains 90% of the total mass of this system. Data come from Run 3, see parameter set-up in Table 1.

On the other hand, Figure 12 shows something interesting with the energy evolution. From the left panel we can see that the cluster undergoes an energy 'burst' during the close approach, which is mainly the burst of kinetic energy. But afterwards the cluster's energy drops down and the cloud's energy rises up, which seems like an energy exchange. We tried to link this with the video we produced, and immediately realized that the kinetic energy burst of the cluster relates with the 'ejection' of stars, which happens slightly after the cluster passes through the cloud's center.

This might be explained as the stars going out of a deep potential well of the cloud. Then there is an increase of both kinetic and potential energy of the cloud, which corresponds to the 'scatter' of gas particles. Basically this should result from an energy transfer from the cluster to the cloud, but the energy seems not conserved in any way (probably because of the simulation errors?), so we were not able to draw any conclusion on this point yet.

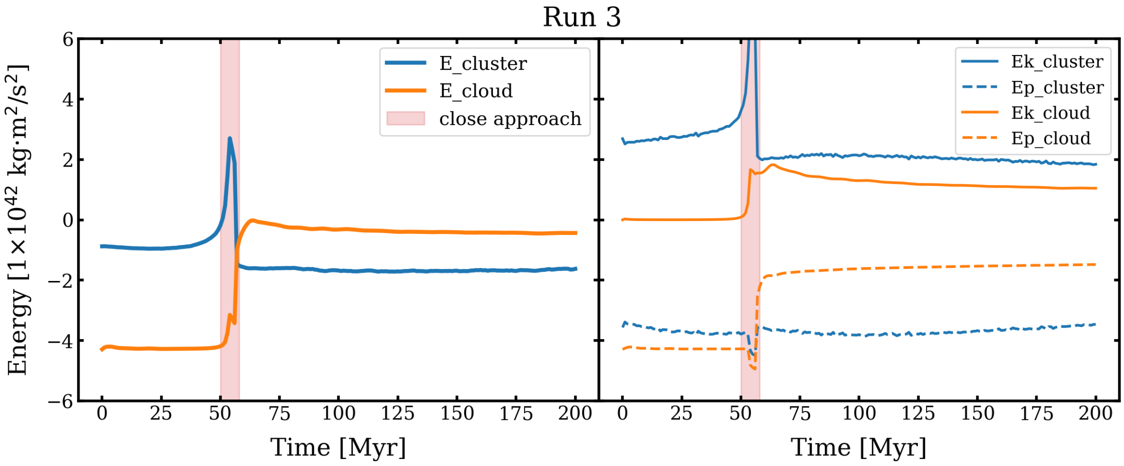

Figure 12: Evolution of total energy (left) and kinetic/potential energy (right) of the cloud and the cluster. Note that all of the energy here is normalized by a factor of 1×10^{42}. Data come from Run 3 as well.

4 Discussion

There are still many improvements that can be done for the future work:

First of all, we are supposed to solve the problem in the bridge between an N-body integrator and the SPH code. This would allow us to simulate the gravitational interaction of the stars more accurately.

Secondly, we could look into exploring the parameter-space of more massive clouds and clusters, since we only talked about the lower end of the mass spectrum in our experiments. However, this would require a significant increase in both computation power and time, therefore the help of super computers is definitely needed.

Thirdly, the initialization of the cloud could also be improved by using more realistic density structures (e.g. the popular filament structures in molecular clouds instead of a simplified Plummer sphere) and more complicated mass distributions for both the cluster and the cloud.

Fourthly, the manner in which the density threshold is calculated could be refined as well. We are currently assuming a constant temperature which should have been specified for each of the gas particles.

Last but not least, we should also dig more into the interaction when the cluster approaches the center of the cloud by increasing the time resolution.

5 Conclusions

We were able to trigger star formation in a collision between a GMC and a globular cluster, but only under some specific conditions:

1. The cluster needs to be massive enough and has a flatter mass distribution (i.e. a large power law index).
2. The cloud needs to contain some regions/gas clumps that have low gravitational stability (e.g. where the local density is already close to the Jeans' density).
3. The cluster should have sufficient time to interact with the dense regions of the cloud, or in other words the relative velocity between the cluster and the cloud should be of moderate value.

By comparing these conditions to the likelihood of encountering them in nature we can try to say something about the probability of a globular cluster triggering star-formation in a GMC. The first two criteria are likely to be met, since true GMCs have far more irregular structures than what we used in our simulation, and it could be possible for the clouds to have some high-density regions. We also used a relatively low-mass globular cluster (due to computational limitations), so it is quite likely that such collisions could occur with far more massive clusters. The last criterion however may be a little bit more difficult to satisfy in nature. We used a low relative velocity of just $10^0 - 10^1$ km/s, while in reality globular clusters can have velocities of up to 300 km/s (Murdin, 2001). But we also justified that the influence of a large relative velocity is not fatal, and it is possible to be compensated by other conditions such as a higher mass of the cluster or the cloud.

References

Dame T. M., Hartmann D., Thaddeus P., 2001, The Astrophysical Journal, 547, 792

Gieles M., Portegies Zwart S. F., Baumgardt H., Athanassoula E., Lamers H. J. G. L. M., Sipior M., Leenaarts J., 2006,] 10.1111/j.1365-2966.2006.10711.x, 371, 793

Jeans J. H., 1902, Philosophical Transactions of the Royal Society of London Series A, 199, 1

Lamers H. J. G. L. M., Gieles M., Bastian N., Baumgardt H., Kharchenko N. V., Portegies Zwart S., 2005,] 10.1051/0004-6361:20042241, 441, 117

Levy V. V., 2000, Astronomical & Astrophysical Transactions, 18, 621

Murdin P. E., 2001, Globular Clusters

Murray N., 2011,] 10.1088/0004-637X/729/2/133, 729, 133

Murray N., Quataert E., Thompson T. A., 2010,] 10.1088/0004-637X/709/1/191, 709, 191

Plummer H. C., 1911, Monthly Notices of the Royal Astronomical Society, 71, 460

Portegies Zwart S., et al., 2019, AMUSE: the Astrophysical Multipurpose Software Environment, doi:10.5281/ZENODO.3260650, `https://zenodo.org/record/3260650#.XZMXFeYzaAk`

Wallin J. F., Higdon J. L., Staveley-Smith L., 1996,] 10.1086/176920, 459, 555